Journal of Physics and Its Applications

Journal homepage : https://ejournal2.undip.ac.id/index.php/jpa/index

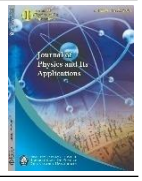

Colloidal TiO_2 Nanoparticles Synthesized via Pulsed Laser Ablation in Liquid for Photocatalytic Degradation of Rhodamine B

Nafaul Mubarokah[1,2], Ali Khumaeni[1,2*], and Iis Nurhasanah[1,2]

[1]*Department of Physics, Faculty of Science and Mathematics, Diponegoro University, Semarang, Indonesia*
[2]*Research Centre for Laser and Advanced Nanotechnology, Diponegoro University, Semarang, Indonesia*

**Corresponding author : khumaeni@fisika.fsm.undip.ac.id*

ARTICLE INFO

Article history:
Received: 1 October 2025
Accepted: 14 December 2025
Available online: 27 February 2026

Keywords:
TiO_2 nanoparticles
Pulsed laser ablation
Photocatalysis
Rhodamine B

ABSTRACT

Colloidal TiO_2 nanoparticles were synthesized via pulsed laser ablation in liquid (PLAL) method using a Q-switched Nd:YAG laser operating at 1064 nm. The optical and structural properties were analyzed using UV-Vis spectroscopy, X-ray diffraction (XRD), and transmission electron microscopy (TEM). XRD confirmed an anatase-dominant nanocrystalline phase. The optical bandgap obtained from the Tauc plot was 3.65 eV. Photocatalytic activity was evaluated through the degradation of Rhodamine B (10 ppm) under UV lamp (254 nm) irradiation. The TiO_2 photocatalyst achieved more than 75% degradation within 150 minutes, whereas the control (photolysis without catalyst) showed less than 5% degradation. These results demonstrate that PLAL enables a clean physical route to produce high-purity anatase TiO_2 nanoparticles with efficient photocatalytic performance.

1. Introduction

Environmental pollution caused by persistent organic dyes, such as Rhodamine B (RhB), poses a serious challenge due to their toxicity, stability, and resistance to biodegradation [1-3]. Photocatalysis using semiconductor materials has become an effective strategy to mineralize such pollutants [4,5].

Among semiconductors, titanium dioxide (TiO_2) remains a benchmark photocatalyst due to its chemical stability, low cost, and strong oxidizing power [6,7]. However, conventional synthesis routes often require chemical precursors or surfactants, leading to impurities. Pulsed Laser Ablation in Liquid (PLAL) provides a clean physical method to generate surfactant-free nanoparticles with tunable size and high purity [8-10].

Beyond eliminating precursor-related contaminants, PLAL offers controllable synthesis parameters, such as laser fluence, pulse duration, wavelength, and the surrounding liquid medium that directly influence nucleation behavior, crystallite size, defect density, and surface chemistry, enabling fine tuning of the physicochemical and electronic properties of TiO_2. Recent developments in TiO_2-based materials have focused on bandgap engineering, defect state control, and surface modification to enhance photocatalytic performance [11-15].

This study reports the synthesis of TiO_2 nanoparticles via PLAL and their photocatalytic degradation efficiency toward Rhodamine B under UV light.

2. Methods

A high-purity TiO_2 target (99.9%) was placed at the bottom of a beaker containing 10 mL of deionized (DI) water. Ablation was performed using a Q-switched Nd:YAG laser operating at a fundamental wavelength of 1064 nm, with a pulse duration of 7 ns, repetition rate of 10 Hz, and pulsed energy of 80 mJ per pulse. The laser beam was directed via mirrors and focused onto the target surface using a focal lens onto the submerged metal target. The ablation process was carried out for 30 minutes under continuous stirring to ensure homogeneous dispersion of the ablated nanoparticles in the liquid medium. The obtained colloid samples were then characterized using UV-Vis and TEM.

The absorption coefficient (α) was determined as:

$$\alpha = \frac{2.303\,A}{d}, \tag{1}$$

where A is the absorbance and d = 1 cm is the optical path length. The optical bandgap was obtained from the Tauc relation:

$$(\alpha h\nu)^2 = A(h\nu - E_g) \tag{2}$$

by plotting $(\alpha h\nu)^2$ vs $h\nu$ and extrapolating the linear region to intercept the photon-energy axis.

A 50 mL RhB solution (10 ppm) was mixed with 10 mL TiO_2 colloid and stirrer in the dark for 60 min to achieve adsorption equilibrium. Irradiation was

carried out under a 24 W UV lamp (λ = 254 nm) for 150 min. UVC light was used to directly excite TiO_2 and evaluate its intrinsic photocatalytic activity. Samples were collected every 30 min and directly analyzed at λmax = 554 nm using a UV-Vis spectrophotometer. Degradation efficiency was calculated as:

$$\eta(\%) = \frac{A_0 - A_t}{A_0} \times 100 \quad (3)$$

where A_0 and A_t are the absorbance values at time 0 and t, respectively.

3. Results and Discussion

3.1. Morphological Analysis

The PLAL process produced an off-white colloidal TiO_2 suspension. TEM images Fig. 1a show mostly near-spherical nanoparticles. The particle size distribution Fig. 1b indicates that the sample is not monodisperse, with particles distributed across several diameter intervals. Approximately 36% of the particles fall in the 10-15 nm range, representing the dominant size population.

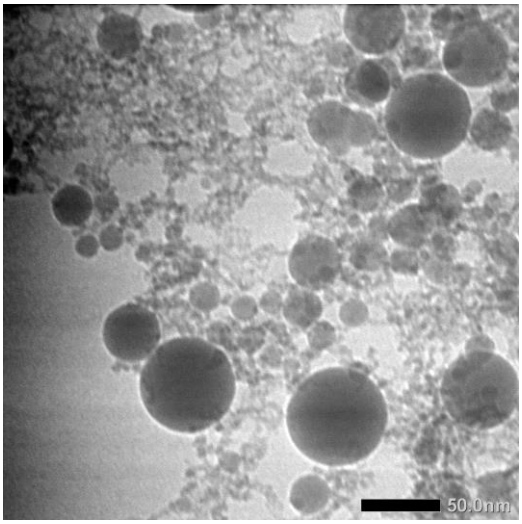

(a)

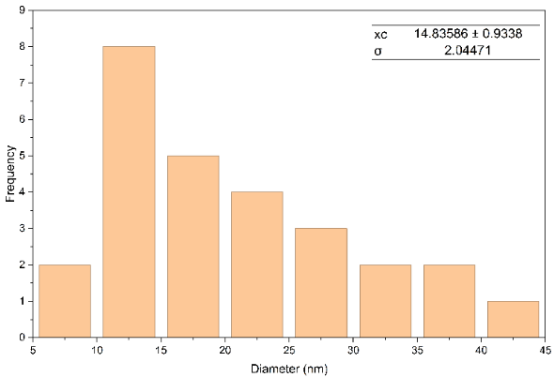

(b)

Fig. 1: (a) TEM images of TiO_2 nanoparticles (b) Particle size distribution histogram obtained from TEM images.

Around 22% are within 15-20 nm, followed by roughly 18% in the 20-30 nm interval. A smaller fraction of particles (≈12%) lies in the 30-40 nm range, and less than 5% exceeds 40 nm. The presence of a tail toward larger particle sizes reflects a degree of polydispersity.

The smaller nanoparticles (<20 nm) are expected to govern the excellent photocatalytic behavior due to their high surface-to-volume ratio, whereas the larger particles may contribute to a slight reduction in effective active surface area [16]. Additionally, larger nanoparticles tend to possess fewer surface defects and lower charge-carrier separation efficiency, which could reduce overall photocatalytic reactivity compared to the dominant smaller size population [17].

3.2. Structural Analysis

The XRD pattern of TiO_2 shown in Fig.2 exhibits a dominant broad peak centered around $2\theta \approx 70°$, which is indexed to the (220) plane of anatase TiO_2 according to JCPDS No. 21-1272. The presence of this peak indicates that the sample tends toward an anatase crystalline structure, even though other anatase reflections are not clearly resolved due to peak broadening and noise.

The broad and low-intensity features observed in the 25-40° region suggest a nanocrystalline domain size, consistent with the TEM-determined particle size of ~15 nm. Such broadening is typical for TiO_2 nanoparticles with crystalline sizes below 20 nm, where reduced domain dimensions reduce peak intensity and increase background scattering. Although the overall pattern does not display sharp and well-defined anatase peaks, the emergence of the peak at 70° provides sufficient evidence that anatase is the prevailing phase in the sample.

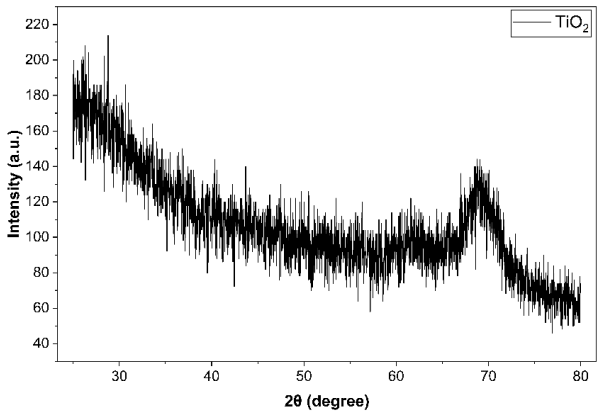

Fig. 2: XRD pattern of TiO_2 nanoparticles

3.3. Optical Properties

The UV-Vis absorption spectrum Fig. 3a shows a clear absorption edge in the near-UV region. Using Eq. (1) and Eq. (2), the Tauc plot Fig. 3b yields an optical bandgap of 3.65 eV, which is slightly higher than that of bulk anatase TiO_2. This blue shift can be attributed to the small crystallite size and reduced long range order of the laser generated nanoparticles.

Nanoparticles synthesized via PLAL typically contain fewer bulk defect states that introduce mid-gap levels, leading to a wider apparent bandgap. The slightly elevated baseline indicates light scattering by suspended nanoparticles, common in colloidal systems [18]. Scattering broadens the absorption edge and can overestimate the apparent bandgap, but its impact remains minor as the main absorption lies in the UV region.

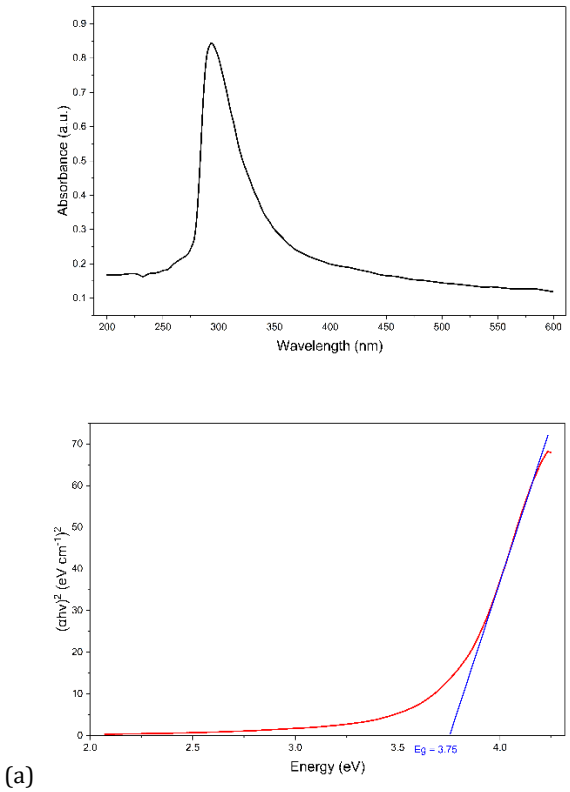

(a)

(b)

Fig. 3: (a) UV-Vis absorbance spectrum of TiO_2 nanoparticles. (b) Tauc plot for bandgap estimation

3.4. Photocatalytic Performance

Fig. 4a shows the progressive reduction of the RhB absorption peak at 554 nm during UV irradiation for 150 min, indicating photocatalytic degradation. The control (without TiO_2) showed less than 5% degradation, confirming minimal photolysis under UV light. In contrast, TiO_2 achieved over 75% degradation within the same duration. The degradation mechanism follows the typical photoactivation pathway of TiO_2 under UV light, which can be described as:

$$TiO_2 + hv \rightarrow e_{CB}^- + h_{VB}^+, \quad (4)$$

The photogenerated electrons and holes subsequently participate in a series of redox reactions that generate reactive oxygen species (ROS) such as •OH and $\bullet O_2^-$. These ROS oxidize RhB through successive N-deethylation and chromophore cleavage, ultimately leading to molecular breakdown. Although the TiO_2 produced via PLAL is nanocrystalline with broadened features, the rapid plasma liquid quenching process introduces a high density of surface hydroxyl groups, under-coordinated Ti sites, and oxygen-related surface defects. These surface features promote dye adsorption and enhance ROS formation, contributing to the observed photocatalytic efficiency. The structural disorder may also induce partial recombination losses, which is consistent with the modest reaction rate.

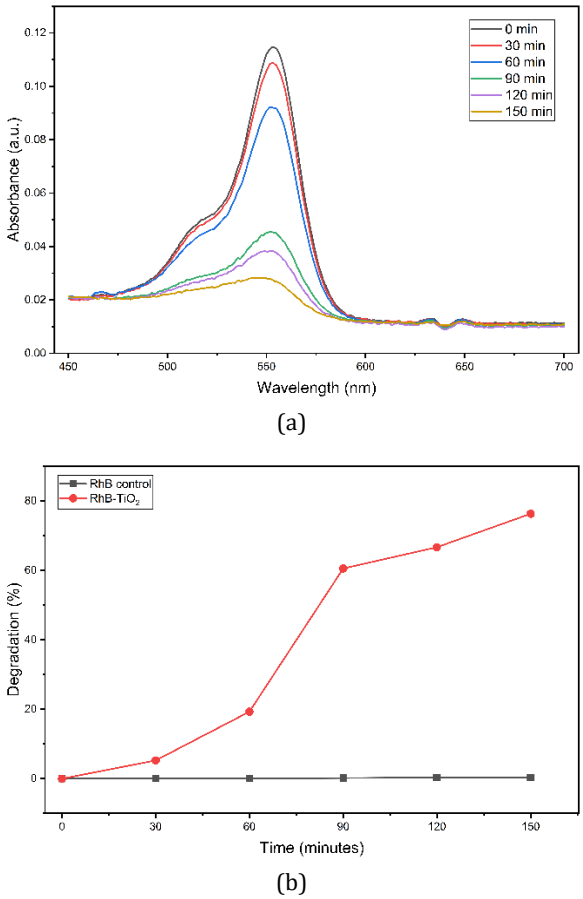

(a)

(b)

Fig. 4: (a) UV-Vis absorbance spectra of Rhodamine B degradation under UV irradiation. (b) Photocatalytic degradation of RhB under UV irradiation compared to the RhB control

This degradation efficiency is within the typical performance range reported for UV-activated TiO_2 nanoparticles, although direct comparison across studies may vary due to differences in irradiation power and experimental configuration.

4. Conclusions

Colloidal TiO_2 nanoparticles were successfully synthesized by PLAL, producing nanocrystalline anatase as confirmed by XRD. The optical bandgap obtained from the Tauc plot was 3.65 eV, consistent with the small crystallite size and reduced long-range order characteristic of laser generated nanoparticles. The TiO_2 colloid demonstrated efficient photocatalytic degradation of Rhodamine B(>75%) within 150 min under UV irradiation, while direct photolysis accounted for <5%. These findings

highlight PLAL as a clean and effective method for producing high purity TiO_2 nanomaterials with promising photocatalytic performance.

Acknowledgment

Part of this work is financially supported by Faculty of Science and Mathematics under World Class University Program of International Collaboration 2025.

References

[1] Y. K. de Souza França, K. S. Pereira, Y. H. C. Feitosa, V. B. Marques, and D. R. de Souza, "Titanium Dioxide (TiO_2) and Photocatalysis: A Detailed Overview of the Synthesis, Applications, Challenges, Advances and Prospects for Sustainable Development," Orbital: Electron. J. Chem., 17(4), 355–381, (2025).

[2] K. Tanaya, A. Kumari, A. K. Singh, and D. Singh, "Bioremediation: An Economical Approach for Treatment of Textile Dye Effluents," Water Air Soil Pollut., 235(8), 516, (2024).

[3] A. K. Al-Buriahi, A. A. Al-Gheethi, P. S. Kumar, R. M. S. R. Mohamed, H. Yusuf, A. F. Alshalif, and N. A. Khalifa, "Elimination of Rhodamine B from Textile Wastewater Using Nanoparticle Photocatalysts: A Review for Sustainable Approaches," Chemosphere., 287(2), 132162, (2022).

[4] H. Wang, X. Li, X. Zhao, C. Li, X. Song, P. Zhang, P. Huo, and X. Li, "A Review on Heterogeneous Photocatalysis for Environmental Remediation: From Semiconductors to Modification Strategies," Chinese J. Catal., 43(2), 178–214, (2022).

[5] A. Krishnan, A. Swarnalal, D. Das, M. Krishnan, V. S. Saji, and S. M. A. Shibli, "A Review on Transition Metal Oxides Based Photocatalysts for Degradation of Synthetic Organic Pollutants," J. of Enviro. Sciences., 139, 389-417, (2024).

[6] S. J. Armakovic, M. M. Savanovic, and S. Armakovic, "Titanium Dioxide as the Most Used Photocatalyst for Water Purification: An Overview," Catalysts., 13(2), 26, (2022).

[7] R. Ghamarpoor, A. Fallah, and M. Jamshidi, "A Review of Synthesis Methods, Modifications, and Mechanisms of ZnO/TiO_2-Based Photocatalysts for Photodegradation of Contaminants," American Chem. Society., 9(24), 25457-25492, (2024).

[8] D. C. Costa, M. Fernandes, C. Moura, G. Miranda, F. Silva, O. Carvalho, and S. Madeira, "Laser Ablation in Liquid-Assisted Synthesis of Three Types of Nanoparticles for Enhanced Antibacterial Applications," Int. J. of Precision Eng. And Manufact.-Green Tech., 12(6), 1699–1717, (2025).

[9] L. V. G. Quinonez, D. C. Garrido, A. C. Hernandez, D. A. A. Leal, G. A. C. Rodriguez, D. F. Gonzalez, E. M. Guerra, M. I. M. Palma, and C. G. Rodriguez, "Synthesis and Characterization of $Bi_4Ti_3O_{12}$ Nanoparticles Obtained via Pulsed Laser Ablation in Liquids," Materials., 16(23), 7451, (2023).

[10] I. Y. Khairani, G. Mínguez-Vega, C. Doñate-Buendía, and B. Gökce, "Green Nanoparticle Synthesis at Scale: A Perspective on Overcoming The Limits of Pulsed Laser Ablation in Liquids for High-Throughput Production," Phys. Chem. Chem. Phys., 25(29), 19380–19408, (2023).

[11] G. Abukhanafer, A. Tiwari, E. Beeram, M. Mariappan, P. R. Dixit, and S. N. Bhavsar, "Photocatalytic Degradation of Organic Pollutants in Water: Application Of Tio_2-Based Nanocomposites," Period. Eng. Nat. Sci., 13(2), 403–416, (2025).

[12] B. Bakbolat, C. Daulbayev, F. Sultanov, R. Beissenov, A. Umirzakov, A. Mereke, A. Bekbaev, and I. Chuprakov, "Recent Developments of Tio_2-Based Photocatalysis in the Hydrogen Evolution and Photodegradation: A Review," Nanomaterials., 10(9), 1790, (2020).

[13] W. L. Hsu, C. W. Tsai, A. C. Yeh, and J. W. Yeh, "Clarifying the Four Core Effects of High-Entropy Materials," Nat. Rev. Chem., 8(6), 471–485 (2024).

[14] N. Riaz, M. Hassan, M. Siddique, Q. Mahmood, U. Farooq, R. Sarwar, and M. S. Khan, "Photocatalytic Degradation and Kinetic Modeling of Azo Dye Using Bimetallic Photocatalysts: Effect of Synthesis and Operational Parameters," Environ. Sci. Pollut. Res., 27(3), 2992–3006, (2020).

[15] S. Rhatigan and M. Nolan, "Insights into Photocatalysis from Computational Chemistry," Heterogeneous Photocatalysis: From Fundamentals to Applications in Energy Conversion and Depollution, 1, 127–154, (2021).

[16] D. Li, H. Song, X. Meng, T. Shen, J. Sun, W. Han, and X. Wang, "Effects of Particle Size on the Structure and Photocatalytic Performance by Alkali-Treated Tio_2," Nanomaterials., 10(3), 546, (2020).

[17] S. Y. Kim, T. G. Lee, S. A. Hwangbo, and J. R. Jeong, "Effect of the Tio_2 Colloidal Size Distribution on the Degradation of Methylene Blue," Nanomaterials., 13(2), 302 (2023).

[18] M. Z. Alhamid, B. S. Hadi, and A. Khumaeni, "Synthesis of Silver Nanoparticles Using Laser Ablation Method Utilizing Nd:YAG Laser" in AIP Conf. Proc., 2202(1), 020013, (2019).